

# Transformation of propagating spin-wave modes in microscopic waveguides with variable width

Vladislav E. Demidov,<sup>\*</sup> Johann Jersch, and Sergej O. Demokritov  
*Institute for Applied Physics, University of Muenster, Corrensstr. 2-4, 48149 Muenster, Germany*

Karsten Rott, Patryk Krzysteczko, and Guenter Reiss  
*Department of Physics, Bielefeld University, P.O. Box 100131, 33501 Bielefeld, Germany*  
 (Received 15 December 2008; revised manuscript received 12 January 2009; published 13 February 2009)

We have studied experimentally the propagation of spin waves in microscopic transversally magnetized permalloy stripe waveguides with variable width. Spatially resolved measurement based on the microfocus Brillouin light-scattering spectroscopy allowed a direct observation of transformations of propagating transverse spin-wave modes in the region of the width transition. Our experiments show that due to the variation in the internal demagnetizing fields caused by the width variation, an effective control of the spin-wave propagation can be achieved. In particular, a splitting of a spin-wave beam into two independent beams or preferred excitation of certain transverse spin-wave modes can be realized.

DOI: [10.1103/PhysRevB.79.054417](https://doi.org/10.1103/PhysRevB.79.054417)

PACS number(s): 75.40.Gb, 75.30.Ds, 75.75.+a, 85.75.-d

## I. INTRODUCTION

Recent developments in the studies of propagating spin waves in microscopic planar ferromagnetic waveguides bring novel possibilities for technical applications of magnetization dynamics in magnetic nanostructures for microwave-frequency signal processing.<sup>1–11</sup> This approach is in many aspects similar to optical signal processing considered within the quickly developing scientific field of plasmon nano-optics.<sup>9</sup> Following the theoretical works on propagation and control of spin waves in microscopic waveguides and complex waveguiding structures,<sup>1,2</sup> this topic has recently received a lot of attention by experimentalists.<sup>3–11</sup> In particular, such phenomena as spin-wave focusing,<sup>4,7</sup> interference,<sup>6</sup> confinement in a nonuniform internal magnetic field,<sup>8–10</sup> and Doppler shift<sup>11</sup> were observed, which create a base for further development of the spin-wave microwave-frequency nano-optics and experimental demonstration of basic signal processing devices, as has been already achieved within the plasmon nano-optics for light-frequency waves.<sup>12</sup> Apart from applications, such investigations are also of fundamental interest, since magnetization dynamics in ferromagnetic nanostructures is strongly affected by both the dipolar and the exchange interactions, as well as by the nonuniformity of the internal magnetic field.

Among the modern measurement methods enabling experimental addressing of spin waves propagating in microscopic structures, the microfocus Brillouin light-scattering ( $\mu$ BLS) spectroscopy (Refs. 13 and 14) is uniquely positioned as the tool which allows direct visualization of spin-wave propagation with submicrometer spatial resolution and high sensitivity.<sup>4,7,9</sup> In fact, due to its ability to provide two-dimensional maps,  $\mu$ BLS spectroscopy is apparently more informative than the widely used spin-wave microwave spectroscopy.<sup>10,11</sup> On the other hand, it is characterized by a significantly wider dynamic range compared to that of time-resolved scanning Kerr microscopy.<sup>3,6,8</sup>

In this work, we use the already mentioned microfocus Brillouin light-scattering spectroscopy to study the propagation of spin waves in microscopic permalloy waveguides with variable width. We show that the variation in the width

of the microwaveguide allows a unique control over the spin-wave propagation regime. In particular, we find that the variation in the demagnetizing field caused by the change in the waveguide width can be used to split a spin-wave beam into two beams independently propagating within a single magnetic stripe, which can be considered as a way to build a spin-wave splitter—the base unit for the realization of a nanoscale spin-wave interferometer. We also find that varying the geometry of the width transition, one gets the possibility to excite transverse spin-wave modes in a controllable way and tune characteristics of the spin-wave focusing effect.

## II. EXPERIMENT

The experimental setup and the investigated samples are sketched in Fig. 1. We studied planar permalloy stripe waveguides with the thickness of 36 nm and the width  $w$  varying from 1.3 to 2.4  $\mu\text{m}$ . The width transition had the length  $L=1, 2, \text{ or } 3 \mu\text{m}$ . The stripes were prepared on a glass substrate by sputter deposition and electron-beam lithography. After the patterning, the stripes were covered by a 25-nm-thick  $\text{SiO}_2$  layer for corrosion protection and electri-

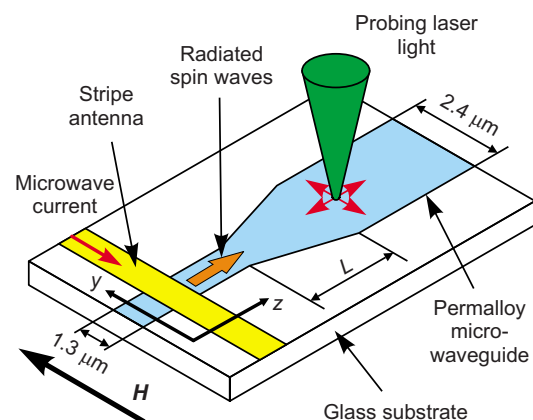


FIG. 1. (Color online) Sketch of the experiment.

cal isolation from an excitation circuit. For local excitation of spin waves, a kind of spin-wave antennae were used. The antennae were made of Au and had the form of  $1.5\text{-}\mu\text{m}$ -wide and  $300\text{-nm}$ -thick stripes. They were oriented perpendicularly to the permalloy waveguides and positioned at a distance of about  $1\ \mu\text{m}$  apart from the start of the width transition. The excitation was performed by means of a single-frequency microwave current transmitted through the antenna. The microwave current produced a local dynamic magnetic field coupled to spin waves, which were radiated in this way and propagated away from the antenna along the magnetic waveguide. The two-dimensional imaging of propagating spin waves was done with the help of  $\mu\text{BLS}$  spectroscopy described in detail elsewhere.<sup>13,14</sup> The  $\mu\text{BLS}$  probing laser light was focused onto the surface of the waveguide and scanned in the two lateral dimensions in order to map spatial distributions of the spin-wave intensity. The experiments were performed for a uniform external magnetic field  $H=1030\ \text{Oe}$  applied in the plane of permalloy waveguides perpendicularly to their axis. This corresponds to the propagation geometry of the so-called Damon-Eshbach mode,<sup>15</sup> which is known for its surface character and the nonreciprocity. However, these features do not reveal themselves in our experiments, probably due to the fact that the thicknesses of the studied films are significantly smaller compared to the wavelength of the waves under consideration.

Figure 2(a) shows the distribution of internal magnetic field  $H_i$  inside of the stripe waveguide. This distribution was calculated for the above-described experimental conditions using the theory developed in Ref. 16, which was widely used to describe the propagation of spin waves in macroscopic magnetic samples and stimulated their application in microwave electronics. As seen from the figure, the variation in the waveguide width leads to a significant modification of the transverse profile of  $H_i$  due to the demagnetizing effects. In particular, in the wider part of the waveguide, the profile exhibits a wide plateau in the middle region, where  $H_i$  is nearly uniform; whereas in the narrower part of the waveguide such a plateau is rather narrow. Besides, the maximum value of  $H_i$  in the middle of the waveguide changes from  $870$  to  $950\ \text{Oe}$ , as the waveguide width changes from  $1.3$  to  $2.4\ \mu\text{m}$ . Such a variation of  $H_i$  is expected to result in a noticeable difference of the spin-wave dispersion spectra. In order to characterize this difference, we calculated the dispersion characteristics for the fundamental spin-wave mode using the theory developed in Ref. 17 taking into account the finite width of the permalloy stripe according to Ref. 18. The results of calculations presented in Fig. 2(b) give a rough estimate of the effect, since they were obtained by a quasia-diabatic approximation for the values of the internal field determined in the middle of the stripe. The figure shows that in the narrow part of the waveguide, the spin-wave dispersion curve is shifted in comparison to that in the wider part by about  $0.5\ \text{GHz}$  toward smaller frequencies, which happens due to the smaller internal magnetic field as well as due to the smaller transverse wavelength. Correspondingly, the lower cut-off frequency of spin waves  $f_{\text{co}}$  also appears to be different for wide and narrow parts of the waveguide. As a result, a region of frequencies exists where the spin waves

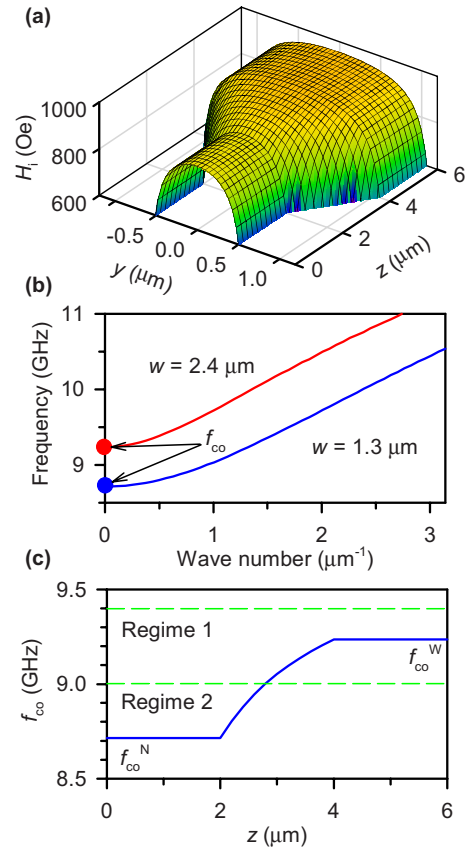


FIG. 2. (Color online) (a) Calculated distribution of the internal magnetic field inside of the permalloy waveguide with variable width. (b) Dispersion characteristics of the fundamental spin-wave mode calculated for the narrow ( $w=1.3\ \mu\text{m}$ ) and wide ( $w=2.4\ \mu\text{m}$ ) parts of the waveguide.  $f_{\text{co}}$ , lower cut-off frequency of the fundamental spin-wave mode. (c) Calculated dependence of the lower cut-off frequency on the propagation coordinate.

can only propagate in the narrower part of the waveguide, but are not allowed to propagate in the wider part. This fact is further illustrated by Fig. 2(c), where  $f_{\text{co}}$  is plotted versus the propagation coordinate  $z$ . Considering the data shown in Fig. 2(c), one can distinguish two essentially different regimes of spin-wave propagation through the region of the width transition. If the frequency of spin waves is larger than both cut-off frequencies  $f_{\text{co}}^N$  and  $f_{\text{co}}^W$  (regime 1), the propagation of the fundamental spin-wave mode is allowed in both parts and the width transition causes the variation in the spin-wave wavelength only. On the other hand, if the spin-wave frequency is positioned between  $f_{\text{co}}^N$  and  $f_{\text{co}}^W$  (regime 2), the character of spin-wave propagation should change drastically. Passing from the narrow to the wide part of the waveguide, the spin-wave beam occupying the entire cross section of the narrow waveguide should be transformed into two independent narrow beams propagating in the edge regions, where the internal magnetic field is reduced due to the demagnetizing effects.<sup>9</sup> A particular case of the regime 2 is the excitation in the wide part of the waveguide of nonpropagating localized modes<sup>19</sup> characterized by a zero wave number in the direction along the waveguide axis, which is possible for lower excitation frequencies than those used in the cur-

rent experiment. However, since here we are interested in transformations of propagating spin waves, localized modes are out of the scope of this paper. In our experiments we studied both above-discussed regimes for propagating spin waves for different lengths of the transition region  $L$ , which (as shown below) determines the characteristics of the transformation of the spin-wave modes.

### III. RESULTS AND DISCUSSION

In the first step, we experimentally determined the cut-off frequencies  $f_{co}^N$  and  $f_{co}^W$ . For this we performed spatially resolved  $\mu$ BLS measurements using fixed-width permalloy stripes and determined the frequency at which the spin-wave propagation changes from the single-beam to the double-beam regime.<sup>9</sup> For the waveguides with the widths  $w=1.3$  and  $2.4 \mu\text{m}$ , these frequencies were found to be 8.4 and 9.2 GHz, respectively. Note that the experimentally found cut-off frequencies differ slightly from those obtained from calculations [see Fig. 2(c)]. This disagreement is explained by the fact that the internal magnetic field in the waveguide is strongly nonuniform, which was not taken into account in the above calculations. As mentioned above, this nonuniformity appears to be much stronger for the narrow stripe than for the wide one [see Fig. 2(a)]. Correspondingly, the disagreement of the measured cut-off frequency from the calculated one is stronger for the narrow stripe. In fact, exact analytical calculation of the dispersion characteristics for spin waves propagating in a nonuniform magnetic field is rather complicated and represents a challenge for theoretical studies in the future.

In the next step, we measured two-dimensional maps of the spin-wave intensity for waveguides with variable width and different length of the width transition applying an excitation current at the frequency  $8.4 < f < 9.2$  GHz, which corresponds to the propagation regime 2 in Fig. 2(c). The results of these measurements for the waveguide with  $L=2 \mu\text{m}$  are presented in Fig. 3. The maps have dimensions of  $2.5$  by  $6 \mu\text{m}$  and were recorded with the spatial step sizes of  $100$  and  $250$  nm in the  $y$  and  $z$  directions, respectively. In order to see the intrinsic spatial structure of the spin-wave beams in Fig. 3, we numerically compensated their spatial decay by normalizing the integral of the measured intensity over transverse sections of the waveguide  $I$  along the propagation coordinate, which corresponds to the normalization of the spin-wave energy flow.

Figure 3 demonstrates that our scenario for the propagation regime 2 can be realized in practice over a wide range of excitation frequencies. In agreement with the theoretical analysis, a single spin-wave beam excited and propagating in the narrow part of the waveguide is split into two beams as the waveguide width increases. Moreover, the distance between the separated beams grows with the decrease in the excitation frequency, which allows their identification as independent beams propagating in the two field-induced channels.<sup>9</sup> Note that the excitation of the two beams is not fully symmetrical. The origin of this slight asymmetry is not clear at the moment. Most probably it originates from a small (about  $2^\circ$ ) misalignment of the stripe antenna.

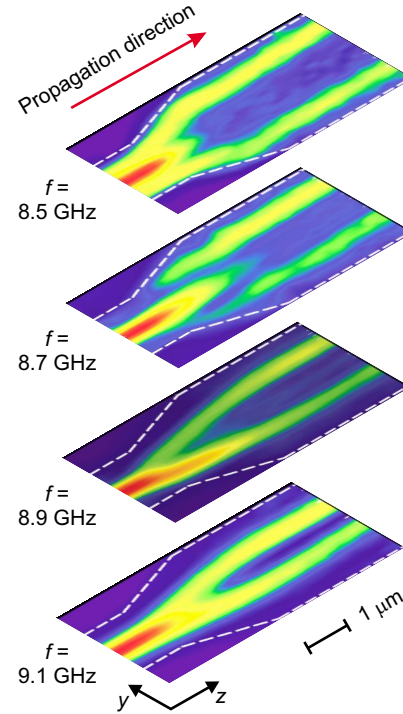


FIG. 3. (Color online) Measured two-dimensional maps of the spin-wave intensity for waveguides with variable width and the length of the width transition  $L=2 \mu\text{m}$  in the propagation regime 2. The maps have dimensions of  $2.5$  by  $6 \mu\text{m}$  and were recorded with the spatial step size of  $100$  and  $250$  nm in the  $y$  and  $z$  directions, respectively. Spatial decay is numerically compensated, as described in the text. Dashed lines show the mechanical boundaries of the waveguide.  $f$ , excitation frequency.

The decay characteristics of the spin-wave beams before and after the splitting are illustrated in Fig. 4, showing the dependence of the transverse integral  $I$  on the propagation coordinate in the logarithmic scale. In the figure, one can

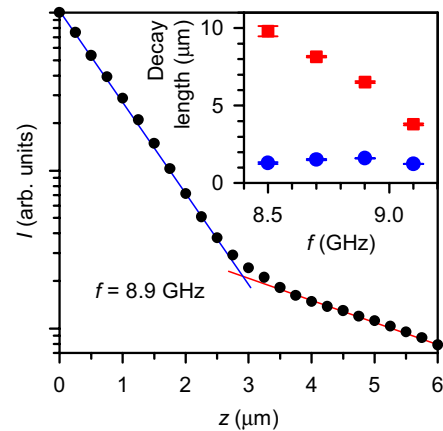


FIG. 4. (Color online) Dependence of the integral of the measured spin-wave intensity over the transverse sections  $I$  on the propagation coordinate (note the logarithmic scale). Inset: decay length of spin waves in the narrow (circles) and wide (squares) parts of the permalloy waveguide as a function of the excitation frequency.

clearly see two regions of exponential decay with significantly different decay rates. It appears that after the splitting of the single spin-wave beam, the spatial decay rate is significantly reduced, which can be associated with much higher group velocity of spin waves propagating in the narrow field-induced channels compared to that of spin waves confined due to the mechanical boundaries of the waveguide. Fitting the data in Fig. 4 by the exponential decay function in both parts of the waveguide, we determined the decay lengths of the spin waves, at which the spin-wave amplitude decreases by a factor of  $e$ , and their dependence on the excitation frequency. These data are shown in the inset in Fig. 4 by circles and squares for the narrow and wide parts of the waveguide, respectively. It is interesting to note that in the single-beam propagation regime the decay length is practically independent of the excitation frequency, whereas in the double-beam regime it changes more than by a factor of 2 over the frequency range of 0.6 GHz. This fact cannot be explained at the moment, since the theory of spin waves guided by field-induced channels is still missing. However, it looks reasonable that the decay length for the double-beam regime approaches that for the single-beam regime as the excitation frequency approaches the critical frequency of 9.2 GHz, at which the transformation of the beams disappears. Figure 4 also demonstrates the very important fact that no spin-wave intensity drop appears in the region of the width transition. From this fact, one can conclude that the spin wave does not experience any significant reflections from the transition region and the energy of the single beam is nearly fully transmitted into the double beams. Note here that—as was found from additional experiments—the variation in the transition length within 1–3  $\mu\text{m}$  does not change the above characteristics of the splitting process significantly. Both these properties of the spin-wave transformation are important for technical applications. In fact, the demonstrated phenomenon can be directly used to build an efficient spin-wave splitter. Moreover, since the nonreciprocity of Damon-Eshbach waves does not play an essential role for such thin films, the subsequent decrease in the waveguide width should result in a backward merge of the split beams. Therefore, simply varying the waveguide width, one can build a microscopic spin-wave Mach-Zehnder interferometer, which has been recently proposed as a key element for the realization of spin-wave logical devices.<sup>20</sup>

Our results show that for practical realization of such an interferometer, it is not necessary to lithographically define two independent waveguiding branches. Instead, one can realize it with one single waveguide with variable width.

Let us now consider another regime of spin-wave propagation [regime 1 in Fig. 2(c)]. As discussed above, if the frequency of the spin wave is larger than both cut-off frequencies in the narrow and wide parts of the waveguide ( $f > 9.2$  GHz), one does not expect any significant changes in the spin-wave propagation except a change in the wavelength. Nevertheless, the experiments performed in this regime also revealed interesting transformations of the spin-wave modes in the transition region. Figure 5 shows the decay-compensated maps of the spin-wave intensities recorded for the frequency  $f=9.7$  GHz, for waveguides with different lengths of the width transition  $L=1, 2,$  and  $3 \mu\text{m}$ .

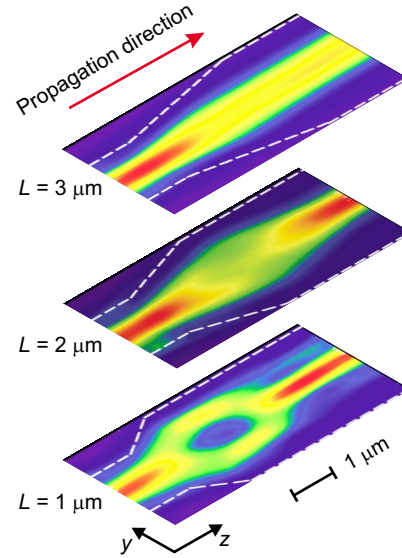


FIG. 5. (Color online) Measured two-dimensional maps of the spin-wave intensity for waveguides with variable width and the length of the width transition  $L=1, 2,$  and  $3 \mu\text{m}$ , as indicated. Excitation frequency  $f=9.7$  GHz, which corresponds to the propagation regime 1. Spatial decay is numerically compensated. Dashed lines show the mechanical boundaries of the waveguide.

As seen from the figure, passing from the narrow to the wide part of the waveguide the spin-wave beam can change noticeably, depending on  $L$ . In particular, for long transitions ( $L=3 \mu\text{m}$ ), the spin-wave beam in the wide part of the waveguide propagates uniformly, not changing its transverse profile with the propagation coordinate. As the transition length is decreased, the beam starts to expand in the region of the width transition and then strongly compresses, demonstrating recently observed spin-wave focusing effect,<sup>7</sup> which becomes more pronounced with the decrease of  $L$ . These changes are further characterized by Fig. 6, where the width of the beam is shown as a function of the propagation coordinate for the waveguides with different  $L$ . In the case of a long transition ( $L=3 \mu\text{m}$ ), the width exhibits an expected increase across the region of the transition and then stays

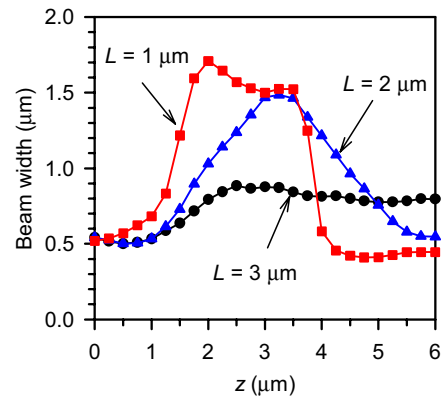


FIG. 6. (Color online) Dependences of the width of the spin-wave beam on the propagation coordinate for different lengths of the transition of the waveguide width  $L$ .

constant over the entire propagation path. For shorter transitions, the width of the beam becomes modulated in space with the depth of the modulation being dependent on  $L$ . In particular, for  $L=2$  and  $1\ \mu\text{m}$ , the modulation of the beam width accounts a value of 90% and 120%, respectively. Note that for  $L=1\ \mu\text{m}$ , the smallest width of the beam in the wide part of the waveguide is equal to 400 nm, which is even smaller than the smallest beam width of 500 nm observed in the narrow part of the waveguide.

To explain these experimental findings, one has to recall that the spin-wave focusing effect is caused by the interference of copropagating spin-wave modes quantized in the transverse direction and its strength is determined by relative intensities of the fundamental and the higher-order modes.<sup>7</sup> In fact, the ratio between these intensities is governed by the geometry of the element used for excitation of spin waves. For the case of a stripe antenna, the higher-order modes are excited with rather small efficiency and the interference leads to moderate modulation and focusing effects.<sup>7</sup> Our present findings show that by using a waveguide with variable width and short width transition, one can excite higher-order modes in a much more efficient way. As seen from Fig. 5 ( $L=1\ \mu\text{m}$ ), this excitation can be so efficient that at a certain propagation distance the fundamental mode is completely suppressed on the axis of the waveguide due to the interference and the spin-wave beam seems to split into two beams. However, one should keep in mind that this splitting effect is essentially different from that observed in the propagation regime 2. Contrary to the previously discussed splitting, the formed beams are coupled to each other. Therefore, a simple

approach for the spin-wave interferometry taking into account only the local value of the field and its gradient<sup>20</sup> cannot be used in this case. Nevertheless, the observed phenomenon of mode transformation can be very useful due to its other features. Since it allows one to controllably excite higher-order spin-wave modes, it provides a way to strengthen the effect of spin-wave focusing and obtain very high concentration of the spin-wave energy in the focal point.

#### IV. CONCLUSIONS

In conclusion, we have demonstrated that due to the variation in the internal magnetic field, the variation in the width of magnetic microwaveguides provides an impressive control over the propagation of spin waves. This is a particular case of their controllability originating from the strong dependence of spin-wave characteristics on the magnetic field, which is one of the most significant advantages of the spin-wave nano-optics in comparison to the plasmon nano-optics. We believe that our experimental findings will further stimulate the development of this direction in microwave nano-electronics, as well as further theoretical investigations of spin-wave propagation in nonuniform magnetic fields.

#### ACKNOWLEDGMENT

This work was supported in part by the Deutsche Forschungsgemeinschaft.

\*Corresponding author; demidov@uni-muenster.de

<sup>1</sup>R. Hertel, W. Wulfhekel, and J. Kirschner, Phys. Rev. Lett. **93**, 257202 (2004).

<sup>2</sup>S. Choi, K.-S. Lee, K. Yu. Guslienko, and S.-K. Kim, Phys. Rev. Lett. **98**, 087205 (2007).

<sup>3</sup>Z. Liu, F. Giesen, X. Zhu, R. D. Sydora, and M. R. Freeman, Phys. Rev. Lett. **98**, 087201 (2007).

<sup>4</sup>V. E. Demidov, S. O. Demokritov, K. Rott, P. Krzysteczko, and G. Reiss, Appl. Phys. Lett. **91**, 252504 (2007).

<sup>5</sup>M. P. Kostylev, G. Gubbiotti, J.-G. Hu, G. Carlotti, T. Ono, and R. L. Stamps, Phys. Rev. B **76**, 054422 (2007).

<sup>6</sup>K. Perzlmaier, G. Woltersdorf, and C. H. Back, Phys. Rev. B **77**, 054425 (2008).

<sup>7</sup>V. E. Demidov, S. O. Demokritov, K. Rott, P. Krzysteczko, and G. Reiss, Phys. Rev. B **77**, 064406 (2008).

<sup>8</sup>V. V. Kruglyak, P. S. Keatley, A. Neudert, M. Delchini, R. J. Hicken, J. R. Childress, and J. A. Katine, Phys. Rev. B **77**, 172407 (2008).

<sup>9</sup>V. E. Demidov, S. O. Demokritov, K. Rott, P. Krzysteczko, and G. Reiss, Appl. Phys. Lett. **92**, 232503 (2008).

<sup>10</sup>J. Topp, J. Podbielski, D. Heitmann, and D. Grundler, Phys. Rev. B **78**, 024431 (2008).

<sup>11</sup>V. Vlaminck and M. Bailleul, Science **322**, 410 (2008).

<sup>12</sup>S. I. Bozhevolnyi, V. S. Volkov, E. Devaux, J.-Y. Laluet, and T. W. Ebbesen, Nature (London) **440**, 508 (2006).

<sup>13</sup>V. E. Demidov, S. O. Demokritov, B. Hillebrands, M. Laufenberg, and P. P. Freitas, Appl. Phys. Lett. **85**, 2866 (2004).

<sup>14</sup>S. O. Demokritov and V. E. Demidov, IEEE Trans. Magn. **44**, 6 (2008).

<sup>15</sup>R. W. Damon and J. R. Eshbach, J. Phys. Chem. Solids **19**, 308 (1961).

<sup>16</sup>R. I. Joseph and E. Schlomann, J. Appl. Phys. **36**, 1579 (1965).

<sup>17</sup>B. A. Kalinikos, IEE Proc., Part H: Microwaves, Opt. Antennas **127**, 4 (1980).

<sup>18</sup>K. Yu. Guslienko, S. O. Demokritov, B. Hillebrands, and A. N. Slavin, Phys. Rev. B **66**, 132402 (2002).

<sup>19</sup>J. Jorzick, S. O. Demokritov, B. Hillebrands, M. Bailleul, C. Fermon, K. Y. Guslienko, A. N. Slavin, D. V. Berkov, and N. L. Gorn, Phys. Rev. Lett. **88**, 047204 (2002).

<sup>20</sup>K.-S. Lee and S.-K. Kim, J. Appl. Phys. **104**, 053909 (2008).